Review of Radio occultation methods for monitoring atmosphere and ionosphere of the earth.

Victor H. Rios, Sebastian Leal y Hernan Esquivel, Physics Department, UNT / UNSTA / CONICET

Abstract

The remote sensing satellite radio occultation method elaborated for monitoring of the earth's atmosphere and ionosphere with a global coverage is described. Comparison of theoretical results with experimental observations of radio wave propagation effects in the earth's atmosphere and ionosphere in the communication links satellite-to-satellite is provided. Directions in application of the radio occultation method are discussed: measuring vertical gradients of the refractivity in the atmosphere and electron density in the lower ionosphere, determination of the temperature regime in the stratosphere and troposphere, investigation of the internal wave activity in the atmosphere, and study of the ionospheric disturbances on a global scale. The radio occultation technique may be applied for investigating the relationships between processes in the atmosphere and mesosphere, study of thermal regimes in the intermediate heights of the upper stratosphere-lower mesosphere, and for analysis of influence of space weather phenomena on the lower ionosphere. Results of radio occultation measurements of the atmospheric and ionospheric parameters are described. Comparative analysis of effectiveness of the radio occultation and other remote sensing methods is conducted.

Introduction

Radio occultation (RO) measurements of the Earth's atmosphere using the GPS constellation and receivers placed on low Earth orbiting (LEO) satellites can provide useful atmospheric profile information (Kursinski et al., 1996; Rocken et al., 1997; Wickert et al., 2001). The technique, which has been widely used in the study of planetary atmospheres (e.g. Fjeldbo et al., 1971), is based on measuring how radio waves are bent by refractive index gradients in an atmosphere.

It can be shown that by assuming spherical symmetry (e.g. Kursinski et al., 1997) this information can be inverted with an Abel transform to give a vertical profile of refractive index and subsequently temperature. The possibility of making RO measurements with a receiver in the atmosphere – probably placed either on a plane or a mountain top – has also been considered by Zuffada et al. (1999). Although fundamentally this is very similar to the LEO measurement, it was originally suggested by Zuffada et al. (1999) that the limits of integration used in the Abel transform meant that it could not be implemented when the receiver is within the Earth's atmosphere and this, in part, led to the development of a more general ray-tracing inversion scheme. (Note that the retrieval scheme outlined by Palmer et al. (2000) could also be applied to this problem.) In fact, an Abel transform can be used in these circumstances. The measurement geometry is similar to that considered by Gaykovich et al. (1983), Beschastnov et al. (1984) and Bruton and Kattawar (1997), who used an Abel transform to invert solar occultation data. Schreiner et al. (1999) also employed the same approach for deriving electron density profiles from ionospheric RO measurements.

1. Radio Occultation Principle (RO)

The theory of RO with a receiver in space has been described in detail by a number of authors (e.g. Melbourne et al., 1994; Kursinski et al., 1997; Rocken et al., 1997). Briefly, the RO technique is based on measuring how radio waves emitted by a GPS satellite are bent by refractive index gradients before being received at a low earth orbiting (LEO) satellite. The geometry is shown in Fig. 1. The LEO is typically ~700 km above the surface of the Earth, whereas the GPS satellite is around 22 000 km above the surface. The receiver on the LEO satellite measures the phase and amplitude of the GPS signal. An excess phase delay is introduced because the neutral atmosphere refractive index is greater than unity and the ray path is curved.

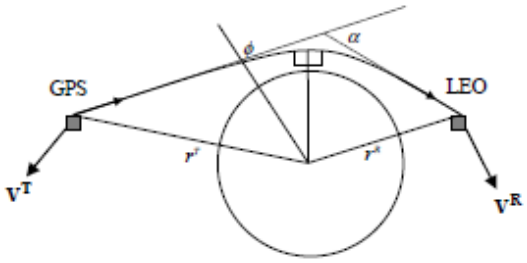

Fig. 1. The geometry of an RO measurement with a receiver on board a LEO satellite.

If the atmosphere is spherically symmetric the bending angle, α, can be written as,

$$\alpha(a) = -2a \int_a^\infty \frac{\frac{d \ln n}{dx}}{(x^2 - a^2)^{1/2}} dx$$

where x = nr. It is a convention in RO to write the upper limit of this integral as infinity, but in practice if the refractive index at, and above, the receiver is effectively unity this can be replaced with r^R, the radius of receiver.
For a spherically symmetric atmosphere, the variation of the corrected bending angle with impact parameter can be inverted with an Abel transform (Phinney and Anderson, 1968; Fjeldbo et al., 1971) to recover the refractive index profile,

$$n(x) = \exp\left(\frac{1}{\pi}\int_x^\infty \frac{\alpha(a)}{(a^2 - x^2)^{1/2}} da\right)$$

which can be evaluated numerically. A useful substitution is a = x cosh α. Once again the upper limit of this integral could be replaced with r^R.
The refractive index can be written as n = 1 + 10^{-6} N, where N is the refractivity. In the neutral atmosphere the refractivity is related to the temperature and the partial pressures of dry air and water vapour pressure T , P_d and P_w through,

$$N = \frac{k_1 P_d}{T} + \frac{k_2 P_w}{T} + \frac{k_3 P_w}{T^2}$$

where k_1 (= 77.60 ± 0.08K/hPa), k_2 (= 70.4 ± 2.2K/hPa) and k_3 (= (3.739±0.012)×105K2/hPa) have been evaluated experimentally (Bevis et al., 1994, and references therein).
The principal RO data characteristic are the global coverage, almost all weather capability; best data quality in upper troposphere - lower stratosphere, with vertical resolution ~ 0.5 km in the troposphere to ~ 1 km up to 30 km, ~ 1-2 km up to stratopause; horizontal resolution ~ 300 km, weather at synoptic scales, gridded atmospheric climatologies; high accuracy of single profiles, temperature < 1 K withn ~ 8-25 km, < 2 K to ~ 4 km and ~ 35km (α, N, p, Z < 1%, 0.5%, 0.3%, 15m). Error characterization of profiles & climatological fields (Scherllin - Pirscher et al., AMT 2011 a, b); structural uncertainty estimates (Ho et al., JGR, 2009); Long - Term stability, measured quantity based on precise atomic clocks; no need of inter-satellite calibration (Foelsche et al., AMT 2011). In fig.2 we show RO - based Climatological Field: F3C-FM4, Dec 2009

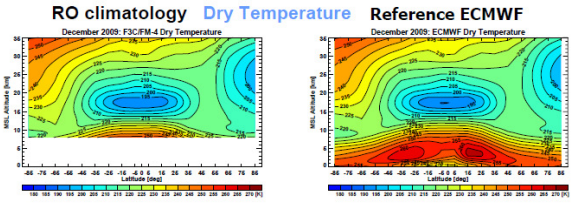

Fig.2 *Comparing RO climatology and Reference ECMWF (Gobiet et al., GRL 2005)*

Other example are the utility of GNSS RO with forecast improvement are show in fig. 3 where GNSS RO key impact on tropical cyclone forecast.

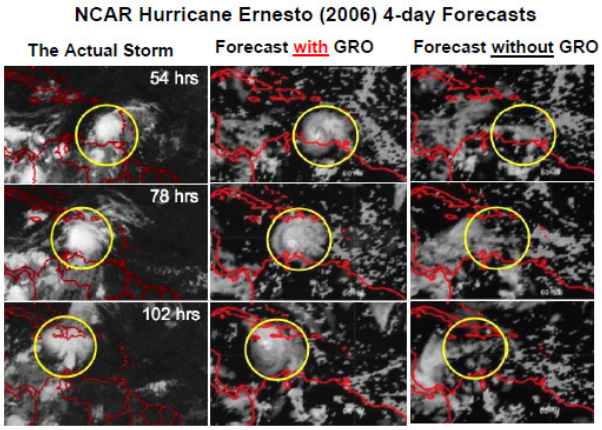

Fig.3 *Tropical cyclone forecast (Liu et al., Mon.Wea.Rev., 2011)*

2. ACE+ and LEO-LEO Occultation Technique

The core part of ACE+ is the novel X/K-band cross-link occultation (LEO-LEO occultation) between pairs of counter-rotating ACE+ satellites measuring the atmospheric refractivity and absorption. ACE+ will actively sound the atmosphere using LEO-LEO signal transmission at three frequencies around the 22 GHz water vapour absorption line (nominally placed near 10, 17, and 23 GHz). Measurements of the occulted phase and amplitude of the electric field from the LEO transmitter at these frequencies will deliver independent information on both humidity and temperature profiles, which will lead to atmosphere data of unprecedented accuracy.

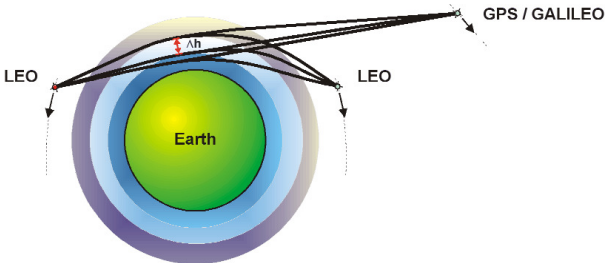

Figure 4 : *Schematic of the observation geometry for LEO-LEO and GPS/GALILEOLEO occultation (Source: Danish Meteorol. Institute).*

The baseline is four satellites in two counter-rotating Sun-synchronous orbits. These orbits should be aligned in the local time of the orbit nodes (equator crossings) with the orbit of the European MetOp satellite series for synergy reasons. A higher orbit (possibly near 800 km) should contain two satellites, while the counter-rotating lower orbit (possibly near 650 km) should contain the other two satellites. Whenever an ACE+ receiver satellite meets over limb an ACE+ transmitter satellite of the other orbit, a rising or setting X/K-band occultation event between the two satellites will occur.

During a LEO-LEO occultation, both the amplitude and phase of the coherent signal will be measured at three different frequencies. Water vapour absorption as function of frequency is not symmetric around the 22 GHz absorption line, and also liquid water contributes to absorption. Utilizing three frequencies can essentially remove the effect of liquid water droplets in clouds from the process of estimating the profiles of tropospheric humidity and temperature. The atmospheric absorption in the relevant frequency range is illustrated in Figure 5.

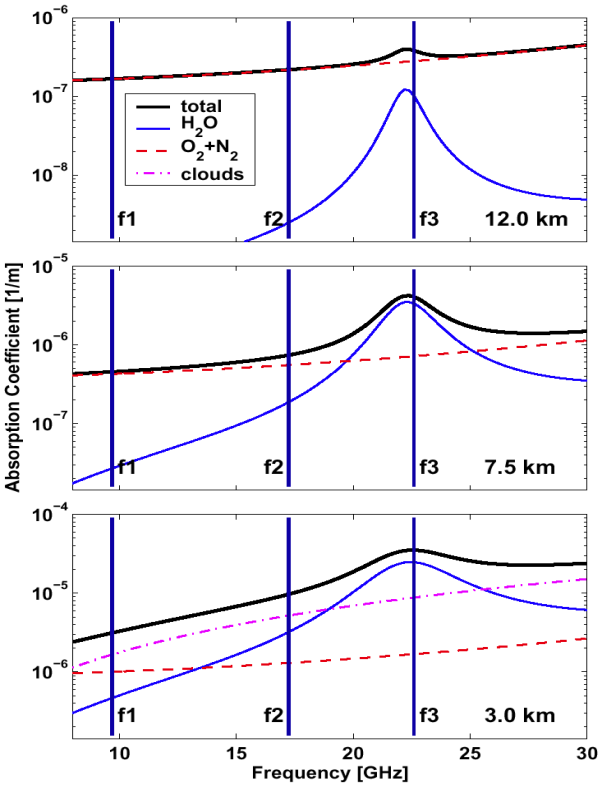

Figure 5: *Atmospheric absorption coefficients as a function of frequency at three different heights (3 km, 7.5 km, 12 km) for a mid-latitude summer atmosphere. The three ACE+ baseline frequencies are indicated. In addition to total absorption, water vapour (H2O), ambient air (O2), and liquid water (cloud; lowest panel) absorption are also shown (Source: Chalmers Univ. of Technology).*

The scientific processing of LEO-LEO occultation data starts from phase and amplitude data, supplemented by the necessary geometric information, and proceeds via Doppler shifts, bending angles, and transmissions down to quasi-vertical atmospheric profiles of real and imaginary refractivities, density, pressure, geopotential height, temperature, humidity, and liquid water. The algorithms consist of the following main steps:
1. bending angle and transmission retrieval,
2. real and imaginary refractivity retrieval,
3. atmospheric profile retrieval.
Bending angle, transmission and refractivity retrievals proceed similar to the GNSSLEO case and will be only briefly addressed below. The emphasis is placed on the description of a tentative atmospheric profiles retrieval processing scheme. More details can be found in Kirchengast et al. (2004a) and Nielsen et al. (2003), with complementary information also to be found, for example, in Kursinski et al. (2002).
Representative performance assessment scenarios based on both a climatological atmosphere and an ECMWF high-resolution analysis field are discussed. The instrumental errors for all scenarios (thermal noise, instrumental 1/f noise, amplitude drift errors) have been modelled according to the defined ACE+ system / instrument requirements. The LEO transmitter and receiver orbits have been assumed consistent with the Phase-A baseline (orbital heights near 650 km and 800 km, etc.). The vertical resolution of the retrieved profiles is ~1 km for all scenarios shown, in line with the respective target requirements

Climatological Atmosphere Cases
A large number of atmospheric scenarios were analysed based on the CIRA86aQ moist-air climatology model (Kirchengast et al. 1999), supplemented by a simple cloud model (Eriksson et al., ESA-ACEPASS study pers. comm. 2003), and an atmospheric turbulence/scintillation model (Sterenborg and Poiares-Baptista, ESA/ESTEC, pers. comm. 2003). Five representative CIRA86aQ cases were defined for this purpose, which together cover humidity and temperature conditions from tropical summer to high-latitude winter. The respective humidity and temperature profiles are illustrated in Figure 6. The scenarios discussed here all use the mid-latitude summer case, results including the other cases are shown by Kirchengast et al. (2004a) and Gradinarsky et al. (2003).

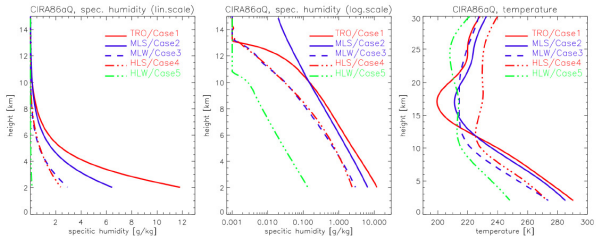

Figure 6: *Humidity and temperature profiles for five representative atmospheric cases of the CIRA86aQ model: tropical (TRO; July 0°N), mid-latitude summer (MLS; July 40°N), mid-latitude winter (MLW, January 40°N), high-latitude summer (HLS, July 70°N), and high-latitude winter (HLW; January 70°N) (Source: Kirchengast et al. 2004b).*

A global set of about 115 occultation events was simulated (the number limited by the computationally expensive forward modelling, as in the previous section), drawing every second event from a day of LEO-LEO measurements, and sorting the events into three latitude bands (low, mid, high). Figure 7 illustrates the coverage by ACE+ LEO-LEO occultation events for a baseline 4-satellite constellation (~230 profiles/day).

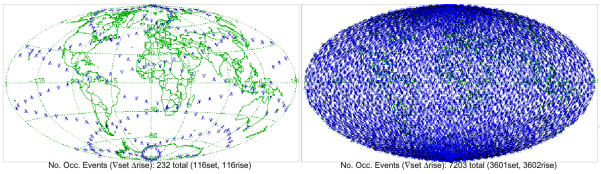

Figure 7: *Coverage by LEO-LEO occultation events for the baseline 4-satellite constellation. Top-left: daily coverage; Top-right: monthly coverage; Bottom: coverage used in the simulations, including every second daily event sorted into low. (Source: Kirchengast et al. 2004b)*

3. Electron density profiles and total electron content

The radio occultation or limb sounding technique and the fundamentals of the global positioning system (GPS) are described in numerous articles, reports and books (e.g., Rocken *et al*., 1997; Lee *et al*., 2001; Melbourne *et al*., 1994; Kaplan, 1996). Remote sensing of the Earth's atmosphere, ionosphere, and oceans by intersatellite links has been rapidly developed since the successful GPS/MET radio occultation mission in 1995–1997. Several new missions are already in orbit (e.g., Oerstedt, SAC-C, CHAMP, GRACE, C/NOFS) or in preparation for launch (e.g., FEDSAT, EQUARS, COSMIC, ACE+). In addition there are some activities, not only to use the decimeter radio waves of GPS but also other wave lengths (e.g., centimeter) which are more sensitive for the measurement of the atmospheric composition (Yakovlev *et al*., 1995). The GPS signals seem to be ideal for active sounding of neutral density and temperature at tropospheric and stratospheric heights and electron density in the ionosphere. Especially the radio occultation data can provide atmospheric profiles of high vertical resolution (1 km to 100 m), mainly depending on the data analysis method (Mortensen *et al*., 1999). There are still some obstacles for the retrieval of electron density profiles from occultation data, since the ionospheric refractivity profile is not so simple as the neutral refractivity profile which exponentially decreases with increase of height and decrease of air density.

In case of the neutral refractivity profile the refraction of the GPS signal mainly occurs within the ray path segment around the tangent point (point of closest approach of the ray to the earth center). Ionospheric refraction of the signal can be significant in all ray path segments, and 'horizontal variations' of the ionosphere over distances of several thousand kilometers should be considered. In the present study we describe the electron density as function of radial distance and geographic position (latitude, longitude). With 'horizontal variation' we always refer to latitudinal and longitudinal variations of electron density at constant radial distance (within a spherical layer).

The launch of the six satellite COSMIC mission in 2005 and numerous other radio occultation missions will lead to a high density of occultation events in space and time. One satellite may collect around 700 ionospheric occultations per day (Hajj *et al*., 2000). We have two methods for reconstruction electron density, 2D and 3D. In 3D, the Abel inversion is applied to each single TEC profile without consideration of horizontal gradients inside the layers. Fig.8 show this reconstruction for midnight and noon at northern summer solstice 23 June 1995 (Hocke and Igarashi, *Earth Planets Space*, **54**, 947–954, 2002)

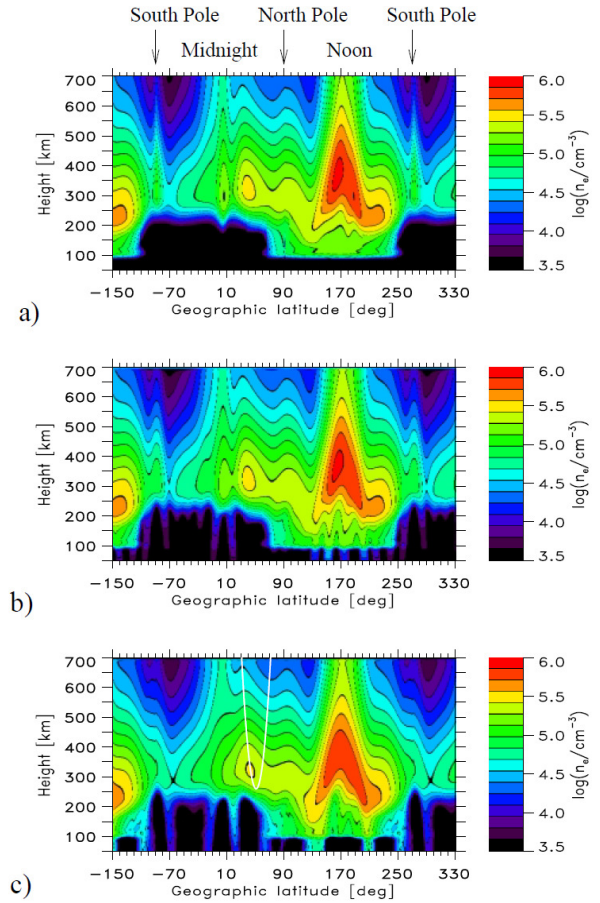

Fig.8: *Reconstruction test of a meridional electron density field from TEC data. a) True IRI-2001 ne field along the Greenwich meridian (0◦ and 180◦ longitude) at midnight and noon at northern summer solstice 23 June 1995 (near to solar minimum), b) Retrieval result of the 2-D recovery method considering horizontal gradients, c) Retrieval result of the Abel inversion (with spherical symmetry assumption). The white line indicates a GPS-LEO ray path through the ionosphere.*

A 2-D recovery method for retrieval of electron density from limb-sounding TEC data has been described. In case of an ideal simulation data set of IRI TEC data this method yields a superior horizontal resolution and accuracy compared to the Abel inversion. For the GPS/MET data set the advantages of this method are questionable, because of the high error propagation along the latitudes for a retrieval in presence of data gaps and TEC errors.

Using COSMIC data, Lei et al. present a ionospheric validation paper COSMIC, which includes publication of the retrieval algorithm by Syndergaard. The plots compare COSMIC measurements of the peak density and altitude in the equatorial ionization anomaly to: an

empirical model (International Reference Ionosphere) (IRI) and a numerical model (NCAR Thermosphere-Ionosphere-Electrodynamics General Circulation Model) (TIEGCM).

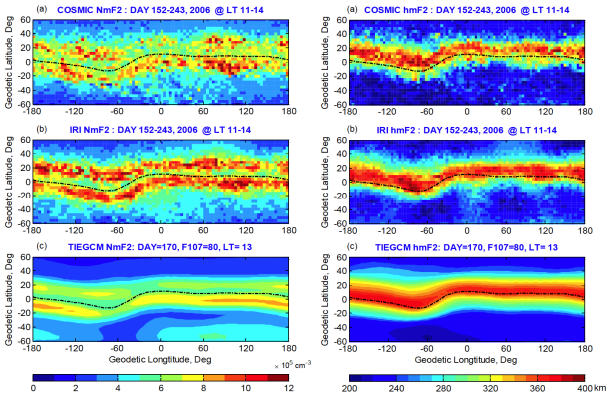

Fig.9: *The plots compare COSMIC measurements of the peak density and altitude in the equatorial ionization anomaly to an empirical model (International Reference Ionosphere) (IRI) and numerical model TIEGCM).*

Now, this is from Zhen Zeng's work on the annual asymmetry in the ionosphere (Fig. 10) . On a global scale, ionospheric densities are higher during northern hemisphere winter than during northern hemisphere summer. This is caused by a combination of the magnetic field tilt and seasonal differences in composition.

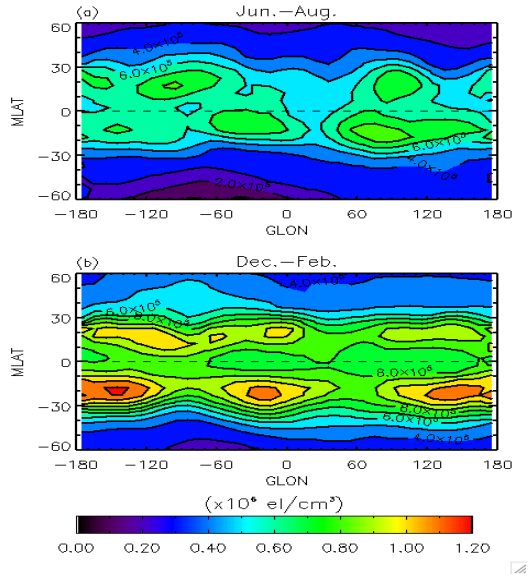

Fig.10 Ionospheric annual asymmetry observed by the COSMIC radio occultation measurements and simulated (Zeng, Z., et al., *J. Geophys. Res.*, *113*, 2008).

Conclusions

This paper proposes the study and development of techniques of the RO techniques. It has been shown how the combination of data of different nature provide with benefits related to the vertical description of the troposphere and ionosphere. It has been shown an improved Abel transform algorithm that uses VTEC data to improve the classical scheme of Abel inversion assuming spherical symmetry. The principal RO data characteristic are the global coverage, almost all weather capability; best data quality in upper troposphere - lower stratosphere, with vertical resolution ~ 0.5 km in the troposphere to ~ 1 km up to 30 km, ~ 1-2 km up to stratopause; horizontal resolution ~ 300 km, weather at synoptic scales, gridded atmospheric climatologies.

A 2-D recovery method for retrieval of electron density from limb-sounding TEC data has been described. In case of an ideal simulation data set of IRI TEC data this method yields a superior horizontal resolution and accuracy compared to the Abel inversion. For the GPS/MET data set the advantages of this method are questionable, because of the high error propagation along the latitudes for a retrieval in presence of data gaps and TEC errors. An additional feature of the proposed improvement of the Abel technique is the treatment of the upper ionosphere and plasmasphere.

References

Bevis, M., Businger, S., Chiswell, S., Herring, T. A., Anthes, R. A., Rocken, C., andWare, R. H.: GPS meteorology: mapping zenith wet delays onto precipitable water, J. Appl. Met., 33, 3, 379–386, 1994.

Beschastnov, S. P., Grechko, G. M., Gurvich, A. S., Zagoruyko, S. V., Kan, V., and Finke, V. V.: Structure of the temperature field from observations of refraction from a high meteorological tower, Izvest. Atmos. and Ocean. Phys., 20, 4, 262–266, 1984.

Born, M. and Wolf, E.: Principles of Optics, Pergamon Press, 6th Edition, 121–124, 1986.

Bruton, W. D. and Kattawar, G. W.: Unique temperature profiles for the atmosphere below an observer from sunset images, Appl. Opt. 36, 27, 6957–6961, 1997.

Fjeldbo, G., Kliore, A. J., and Eshlemann, V. R.: The neutral atmosphere of Venus studied with the Mariner V radio occultation experiments, Astron. J., 76, 2, 123–140, 1971.

Foelsche, U, et al. (2011), Refractivity and temperature climate records from multiple radio occultation satellites consistent within 0.05%, *Atmos. Meas. Tech.*, 4, 2007–2018, doi:10.5194/amt-4-2007-2011, http://www.atmos-meas-tech.net/4/2007/2011/amt-4-2007-2011.html.

Gaykovich, K. P., Gurevich, A. S., and Naumov, P.: On a reconstruction of meteorological parameters from intra-atmospheric measurements of optical refraction of cosmic sources, Izvest. Atmos. and Ocean. Phys., 19, 7, 507–511, 1983.

Gobiet, A., U. Foelsche, A. K. Steiner, M. Borsche, G. Kirchengast, and J. Wickert (2005), Climatological validation of stratospheric temperatures in ECMWF operational analyses with CHAMP radio occultation data,

Geophys. Res. Lett., 32, L12806, doi: 10.1029 /2005GL022617.
Haase, J.: Microearthquake studies in the Anza seismic gap. Ph. D. Thesis, University of California, San Diego, CA, 1992.
Hajj, G. A. and Romans, L. J.: Ionospheric electron density profiles obtained with the Global Positioning System: Results from the GPS/MET experiment. Radio Science, 33, 1, 175–190, 1998.
Healy, S. B. and Eyre, J. R.: Retrieving temperature, water vapour and surface pressure information from refractive-index profiles derived by radio occultation: A simulation study. Q.J.R.Meteorol.Soc., 126, 1661–1683, 2000.
Healy, S. B.: Radio occultation bending angle and impact parameter errors caused by horizontal gradients in the troposphere: A simulation study. J. Geophys. Res. 106, D11, 11 875–11 889, 2001.
Ho, S.-P., et al. (2009), Estimating the uncertainty of using GPS RO data for climate monitoring: Intercomparison of CHAMP refractivity climate records 2002 to 2006 from different data centers, *J. Geophys. Res.*, 114, D23107, doi:10.1029/2009JD011969
Kursinski, E. R., Hajj, G. A., Bertiger, W. I., Leroy, S. S., Meehan,T. K., Romans, L. J., Schofield, J. T., McCleese, D. J., Melbourne, W. G., Thornton, C. L., Yunck, T. P., and Eyre, J. R.: Initial results of radio occultation of the Earth's atmosphere using the Global Positioning System. Science, 271, 1107–1110, 1996.
Kursinski, E. R., Hajj, G. A., Hardy, K. R., Schofield, J. T., and Linfield, R.: Observing Earth's atmosphere with radio occultation measurements using GPS. J. Geophys. Res., 102, D19, 23 429– 23 465, 1997.
Kursinski, E. R. and Hajj, G. A.: A comparion of water vapor derived from GPS occultations and global weather analyses. J. Geophys. Res., 106, D1, 1113–1138, 2001.
Lesne O., Haase, J., Kirchengast, G., Ramsauer, J., and Poetzi, W.: GNSS radio occultation for airborne soundings of the tropopshere: Measurement sensitivity analysis. Submitted to Phys. Chem. of the Earth, 2001.
Melbourne, W. G., Davis, E. S., Duncan, C. B., Hajj, G. A., Hardy, K. R., Kursinski, E. R., Meehan, T. K., Young, L. E., and Yunck, T. P.: The application of GPS to atmospheric limb sounding and global change monitoring, *JPL Publ., 94–18*, 1994.
Phinney, R. A. and Anderson, D. L.: On the radio occultation method for studying planetary atmospheres. J. Geophys. Res., 73, 5, 1819–1827, 1968.
Palmer, P. I., Barnett, J. J., Eyre, J. R., and Healy, S. B.: A nonlinear optimal estimation method for radio occultation measurements of temperature, humidity and surface pressure, J. Geophys. Res., 105, D13, 17 513–17 526, 2000.
Rocken C., Anthes, R., Exner, M., Hunt, D., Sokilovskiy, S., Ware, R., Gorbunov, M., Schreiner, W., Feng, D., Herman, B., Kuo, Y. H., and Zou, X.: Analysis and validation of GPS/MET data in the neutral atmosphere, J. Geophys. Res., 102, D25, 29 849– 29 866, 1997.
Scherllin-Pirscher, B., et al. (2011a), Empirical analysis and modeling of errors of atmospheric profiles from GPS radio occultation, *Atmos. Meas. Tech.*, 4, 1875–1890, doi:10.5194/amt-4-1875-2011, http://www.atmos-meas-tech.net/4/1875/2011/amt-4-1875- 2011.html.
Scherllin-Pirscher, B., et al. (2011b), Quantifying uncertainty in climatological fields from GPS radio occultation: An empiricalanalytical error model, *Atmos. Meas. Tech.*, 4, 2019–2034, doi:10.5194/amt-4-2019-2011, http://www.atmos-meastech. net/4/2019/2011/amt-4-2019-2011.html
Schreiner, W. S., Sokolovskiy, S. V., Rocken, C., and Hunt, D. C.: Analysis and validation of GPS/MET radio occultation data in the ionosphere, Radio Science, 34, 4, 949–966, 1999.
Steiner, A. K., et al. (2009b), Atmospheric temperature change detection with GPS radio occultation 1995 to 2008, *Geophys. Res. Lett.*, 36, L18702, doi:10.1029 /2009GL039777.
Steiner, A. K., et al. (2011), GPS radio occultation for climate monitoring and change detection, *Radio Sci.*, doi:10.1029/2010RS004614, in press
Vorob'ev, V. V. and Krasil'nikova, T. G.: Estimation of the accuracy of the atmospheric refractive index recovery from Doppler shift measurements at frequencies used in the NAVSTAR system.
Physics of Atmosphere and Ocean, 29, 5, 602–609, 1994.
Wickert, J., Reigber, C., Beyerle, G., Konig, R., Marquardt, C., Schmidt, T., Grunwaldt, L., Galas, R., Meehan, T. K., Melbourne, W. G., and Hocke, K.: Atmosphere sounding by GPS radio occultations: First results from CHAMP, Geophys. Res. Lett., 28, 3263–3266, 2001.
Zuffada, C., Hajj, G. A., and Kursinski, E. R.: A novel approach to atmospheric profiling with a mountain-based or airborne receiver, J. Geophys. Res. 104, D20, 24435–24447, 1999.

Acknowledgments
The authors wish to express their gratitude to INCTGP, PETROBRAS, FINEP, FAPESB and PRH8-ANP, for financial support.